The Effect of Branching on Chain Diffusion in Ultralong n-Alkane Crystals Observed by ^{13}C NMR

Martin A. N. Driver and Philip G. Klein*

IRC in Polymer Science and Technology, University of Leeds, Leeds, West Yorkshire, LS2 9JT, United Kingdom

Summary

^{13}C NMR progressive saturation measurements are used to investigate solid state chain diffusion in semicrystalline alkanes. Monodisperse, ultralong n-alkanes, of 198 and 191 carbon atoms in length, are characterized and prepared in such a way that they comprise crystals containing chains which are exclusively of once-folded conformation. This preparation is confirmed with DSC and SAXS. The progressive saturation experiments show that the longitudinal relaxation of magnetisation is consistent with a solid state chain diffusion process. Reptation and one-dimensional diffusion models are demonstrated to satisfactorily represent the data. The addition of branches to the alkane chains is shown to result in a decrease in the diffusion coefficient. The obtained diffusion coefficients range from 0.0918 nm^2s^{-1} for the linear chain to 0.016 nm^2s^{-1} for a chain with a branch 4 carbons in length. These diffusion coefficients are consistent with those previously obtained for polyethylenes.

Introduction

In polymer melts chain diffusion is an important dynamic process. It determines, for example, their viscoelastic and transport properties[1]. Below the glass transition, T_g, in polymers, such diffusion is strongly quenched. Semicrystalline systems where the amorphous phase is above the glass transition temperature are not uncommon. Polyethylene at room temperature is an example of such. Diffusion of chains between the crystalline and amorphous phases would be an important process in these systems, particularly with respect to crystallization, lamellar thickening and annealing phenomena.

 CCC 1022-1360/99/$ 17.50+.50/0

Chain diffusion is significant for the interpretation of longitudinal ^{13}C relaxation in NMR of semicrystalline polymers. Longitudinal relaxation, T_1, is traditionally described as a spin-lattice interaction, whereby nuclei relax via interactions with the surrounding spin system as a whole. This relaxation should be modeled as a single exponential. The ^{13}C decay in the crystalline regions, however, has been observed to be non-exponential[2]. There has also been observed a very large range of crystalline T_1 values for polyethylene, 40-4500s[2]. The apparent ^{13}C T_1 is strongly dependent on morphological and structural factors such as lamellar thickness[2], branching[3] and crosslinking[4] . None of these observations can be explained in terms of a simple spin-lattice interaction.

When the concept of ^{13}C magnetisation transport between the crystalline and amorphous phases was first reported it was considered as a spin diffusion effect, analogous to that observed for ^1H $T_{1\rho}$ relaxation[5]. However, with ^{13}C nuclei being only about 1% naturally abundant, doubts were raised about the feasibility of spin diffusion as the sole transport process.

Subsequently, longitudinal relaxation measurements in polyethylene were interpreted as long distance solid-state chain diffusion between the crystalline and amorphous regions[6]. It was proposed that T_1 relaxation is not the dominant mechanism for recovery of magnetisation within the crystalline regions. Owing to their greater mobility, the amorphous regions relax much more quickly than do the crystalline regions. Nuclei in the crystalline phase diffuse out into the amorphous phase where they relax fully. The amorphous phase thus acts as a sink for magnetisation. These relaxed nuclei then diffuse back into the crystal, where they appear as relaxed crystalline nuclei. The "T_1" which is experimentally measured is not, therefore, representative of the spin-lattice relaxation within the crystal. Rather, it is the diffusion time for a crystalline nucleus to reach the amorphous phase.

As well as being consistent with the observed dependencies of T_1 on morphological aspects[2-4], some direct evidence for this process has been observed[6]. Nuclear Overhauser enhancement measurements suggest that all the magnetisation relaxes by

the same mechanisms, and that the motions leading to this relaxation are consistent with the amorphous phase. 2D exchange NMR experiments have shown detected chain translations between the different phases of polyethylene. The mechanism for this transport has been ascribed to a chain jump process, the α relaxation. This motion involves rotation and translation by one repeat unit[7-8].

This interpretation of ^{13}C T_1 relaxation measurements allows NMR to probe ultraslow chain motion on the timescale of seconds. In this work, such an interpretation will be used to investigate the effect of specific changes in the molecular architecture on the diffusion process. Polymers are generally polydisperse. This leads to uncertainty as to how many folds are formed in the crystal phase, how long any cilia are, how many tie molecules there are and what the branching is like. Since any such morphological effects are important to chain diffusion, this is clearly not ideal. The materials used here are n-alkanes of strictly uniform length. These were first produced in an investigation aimed at elucidation of the chain folding crystallization process[9]. The alkanes used here are the linear alkane $C_{198}H_{398}$, and the branched alkanes $C_{94}H_{190}$-$CH(CH_3)$-$C_{96}H_{194}$ (methyl branch) and $C_{94}H_{190}$-$CH(C_4H_{10})$-$C_{96}H_{194}$ (butyl branch). The work reported here forms part of a wider study involving monodisperse alkanes of various molecular weights (e.g. $C_{246}H_{484}$, $C_{294}H_{590}$), which have been prepared by Dr. G. M. Brooke and co-workers at the University of Durham[10].

With such monodisperse samples, the exact size of each molecule is known as is the size, position and number of branches. Alkane crystals can be produced which contain one fold per chain, with, in the case of the branched samples, the branches at the fold surface, see Fig. 1. With such well characterized morphologies, the ^{13}C NMR measurements of the crystalline relaxation of magnetisation would allow a greater understanding of the nature of the obstacle presented to the chain diffusion process by branching.

Fig. 1: A schematic representation of the folded chain crystals formed by linear and branched alkanes.

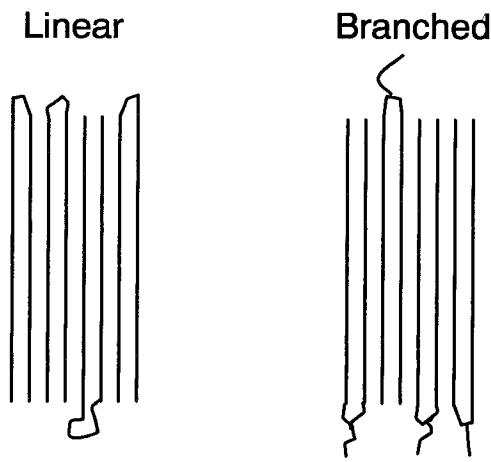

Experimental

High Resolution ^{13}C NMR: Spectra were recorded on a Chemagnetics CMX-200, operating at 200MHz for protons and 50.3MHz for carbons. A progressive saturation pulse sequence was employed, see Fig. 2. A double resonance MAS probe was used, and samples were spun at about 3.5kHz. A 4 μs 90° pulse was used in the ^{1}H and ^{13}C channels, with a decoupling field equivalent to 82 kHz applied during the acquisition period. A series of FIDs were recorded, with a variation in the recycle delay time between 2 and 1200 s. All the experiments were performed at 60°C, as this temperature was believed to represent the ideal conditions for the observation of chain diffusion[6].

Fig. 2: Progressive saturation pulse sequence used to measure the ^{13}C longitudinal relaxation.

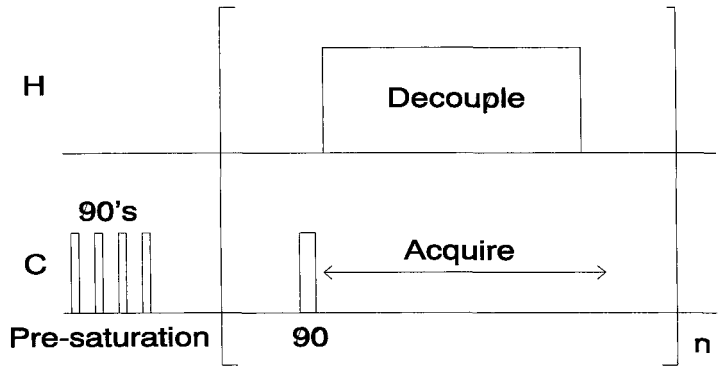

The data lengths of the FIDs were doubled by zero filling, and the signal to noise improved by multiplication of the FIDs by matched exponential filters[11]. They were then Fourier transformed into the frequency domain, where they were baseline corrected to a third order polynomial.

Wideline ^1H NMR: The probe had a 5 mm coil and a pulse width of 2 μs was used. A standard 90x-τ-90y solid echo pulse sequence was used, with interpulse spacing, τ, varying between 7 μs and 30 μs. The broad component of the spectrum, representing the crystalline phase was fitted to a modified Gaussian[4]. The narrow component, representing the mobile amorphous phase, was fitted to a Lorentzian. Each of these components decayed in a Gaussian manner as functions of τ, and was extrapolated back to zero τ to obtain the crystallinity[4]. This was calculated to be 76.2%±2%, 82.6%±2% and 82.3%±2% for the folded linear, methyl branched and butyl branched samples respectively. When annealed to form extended chains the linear alkane's crystallinity was 87.6±2%.

Differential Scanning Calorimetry (DSC): A Perkin-Elmer DSC-7 was used. Experiments were performed at a constant heating or cooling rate of 10°C per minute. Temperature and energy were calibrated from the melting behaviour of two standards, indium and zinc, heating at 10°C per minute.

Small Angle X-Ray Scattering (SAXS): The experiments were carried out on Station 8.2 of the Daresbury Synchrotron Radiation Source. A Daresbury quadrant multiwire detector was used. The correction for positional nonlinearity of the quadrant detector was done using the first 22 orders of diffraction from wet rat tail collagen. A sixth order polynomial was fitted to the inverse collagen spacings over the detector range. All diffraction intensities were normalised by the beam flux which was monitored by an ionisation chamber located behind the specimen.

Results and Discussion

1. Sample Preparation and Characterisation

1(a). DSC

Previous work by other authors on these alkane samples has revealed that they show a preference for crystallizing with quantised fold length, chains completing almost exactly one, two, three or four folds up to the longest chain examined, $C_{390}H_{782}$ [9, 12-14]. This quantisation led to discontinuities in the dissolution temperature. Fig. 3a shows a DSC thermograph of $C_{198}H_{398}$ on cooling from the melt at 10°C per minute. Two distinct crystallization exotherms are visible, corresponding to the formation of extended and once-folded chain material.

Fig. 3: DSC thermographs of alkanes. 3(a) shows a cooling scan of the linear alkane, cooling at 10°C per minute. 3(b) is a heating scan of the linear alkane, subsequent to its being quenched from the melt, heating at 10°C per minute. 3(c) is a heating scan of the methyl branched sample, heating at 10°C per minute.

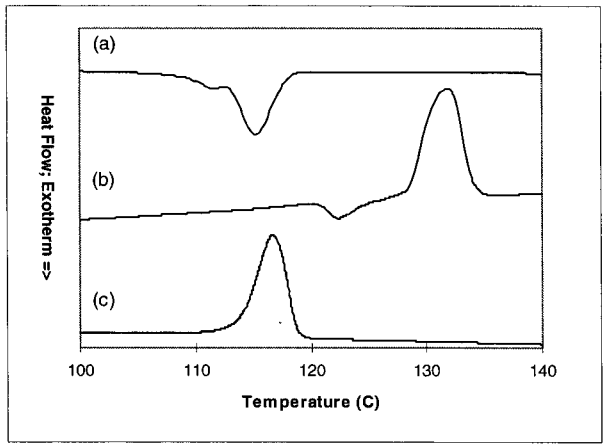

Fig. 3a shows a cooling scan of the linear alkane. Two distinct exotherms are visible, at 112°C and 114°C, corresponding to formation of folded and extended chain material respectively. In an attempt to produce a sample of $C_{198}H_{398}$ which was exclusively made up of folded chain crystals, the material was melted on a hot plate at 150°C, then quenched in liquid nitrogen. Fig. 3b is the DSC scan of this sample heated at 10°C per minute. Initially, around 120°C, a melting endotherm is observed. This corresponds to folded chain material. Subsequently, a thickening exotherm is observed, at 122°C followed by the melting peak for extended chain material at 131°C. Clearly, folded chain crystals have been formed, but it cannot be ascertained from calorimetry whether or not the sample was made up of exclusively folded chain crystals, as these thicken to extended chain crystals during the scan. The melting endotherm of the folded chain crystals is weak because it is superimposed on the exotherm corresponding to the crystallisation of the extended chains.

Fig. 3c is a thermograph of the butyl branched sample. This shows only one peak at 117°C, corresponding to folded chain crystals. Each of the branched samples was only ever observed to show one endotherm, regardless of the crystallisation conditions. The crystals formed comprise once folded chains with the branch point at the fold surface.

1(b). Small Angle X-Ray Scattering (SAXS)

SAXS patterns were recorded for two differently prepared $C_{198}H_{398}$ samples. One was quenched from the melt in an attempt to produce folded chains as described above, the other annealed for 5 minutes at 119°C in an attempt to produce extended chain crystals. These patterns are displayed in Fig. 4.

Fig. 4: SAXS patterns from annealed and extended $C_{198}H_{398}$. The annealed sample shows peaks corresponding to extended chain crystals. The quenched sample shows peaks corresponding to once folded chains.

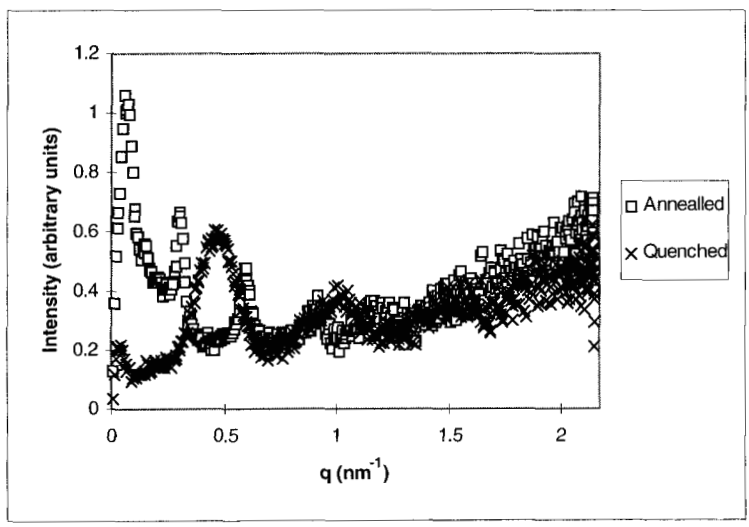

The peak at lowest q is the signal at the edge of the beam stop. The first order annealed peak is at about 0.3 nm^{-1}, the first order quenched peak is near to 0.5 nm^{-1}. It should be noted that these peaks arise from the long spacing, not the lamellar thickness. The spacings are evaluated by treating the data purely as Bragg scattering, i.e. using

$$q = \frac{2\pi}{d} \qquad (1)$$

The calculated long spacings are 20.8 nm for the annealed sample and 12.8 nm for the quenched sample. These are in accordance with values one would calculate for extended chain and once folded chain crystals, from knowledge of the length, geometry, and crystallinity of the alkane, assuming a simple lamellar series morphology. The peaks from the once folded chains do not lie exactly on alternate peaks from the extended chains because the long spacing has been measured and the folded material has a larger interlamellar amorphous phase. This can be asserted following ^{1}H NMR measurements which show the annealed sample to be of higher crystallinity, 87.6% compared to 76.2% for the quenched sample. Quenching the sample in this manner can therefore be safely assumed to produce predominantly once folded chain crystals of the linear alkane.

The SAXS peaks from both the branched samples are also consistent with chains in a once folded conformation, as expected from the DSC results. Fig. 5 shows these scattering patterns.

Fig. 5: SAXS patterns from the methyl and butyl branched samples.

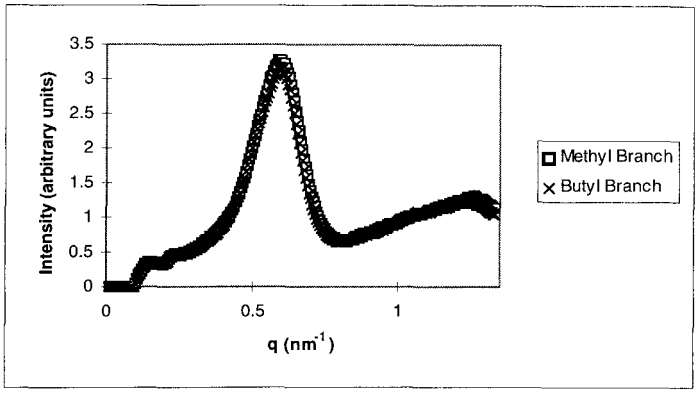

2. ^{13}C NMR Longitudinal Relaxation

In each spectrum four distinct peaks are visible. These are the crystalline peak at 32.5ppm, the amorphous peak at 31ppm, the methyl end group at 13.5ppm and the penultimate carbon at 24ppm. The absorption intensity of the amorphous resonance, and those of the end groups, remains approximately constant over the complete range of recycle times (Fig. 6a). This indicates that the amorphous magnetisation is fully relaxed within 2 seconds, the shortest recycle delay time. In contrast, the crystalline signal increases in intensity over the complete range of recycle times (Fig. 6b). This slow growth in intensity indicates that the crystal phase takes a long time to recover its equilibrium magnetization.

Fig. 6a: ^{13}C NMR spectra for the methyl branched sample, recycle delay times between 2 s and 20 s. The absorption intensity of the amorphous phase, and that of the end groups, remains approximately constant over the full range of recycle delay times.

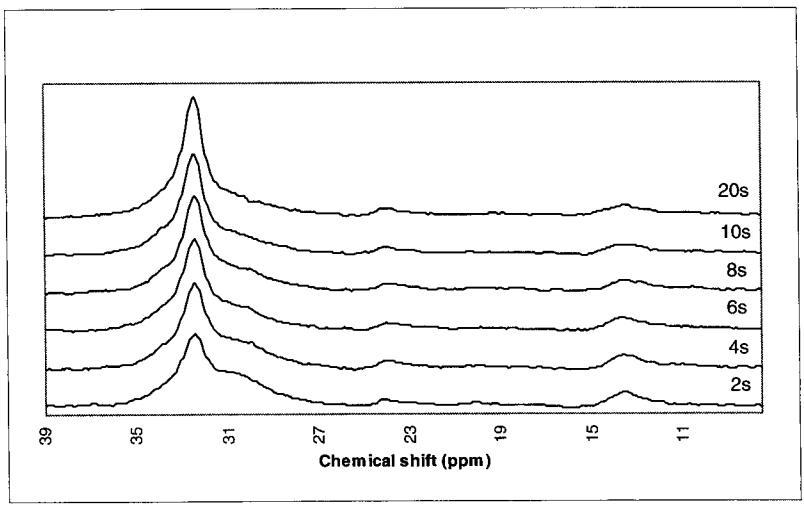

Fig. 6b: ^{13}C NMR spectra for the methyl branched sample, recycle delay times between 2 s and 1200 s. The crystalline signal increases in intensity over the complete range of recycle times

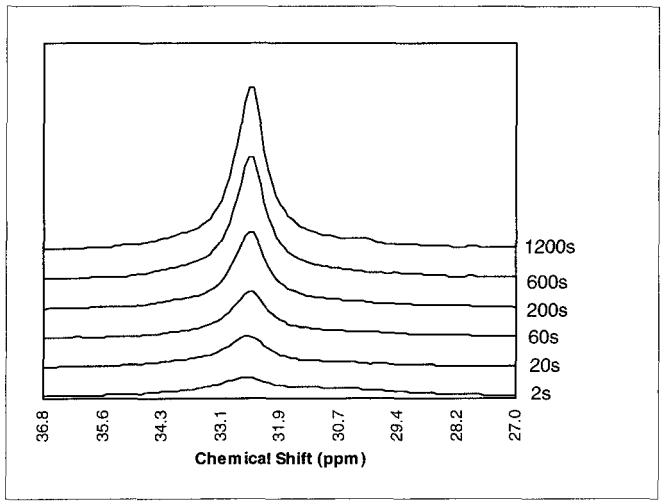

The invariance of the amorphous signal in the ^{13}C NMR spectrum is used as a reference to calculate the growth in the intensity of the crystalline resonance. The evolution of magnetisation can be represented as a fraction of the maximum crystal signal[4].

$$\frac{M(t)}{M_0} = \frac{f_C(t)}{1-f_C(t)} \frac{1-F_C^H}{F_C^H} \qquad (2)$$

Here, M(t) is the longitudinal magnetisation at time t, M_0 is the equilibrium magnetisation, f_C is the fraction of the crystal resonance in ^{13}C NMR spectrum and F_C^H is the crystallinity as measured by deconvolution of the ^1H wideline spectrum. The best fit to the spectra was found by fitting a Lorenztian to the crystalline peak and a Gaussian to the amorphous and end group peaks. A typical example of this sort of fit is shown in Fig. 7.

Fig. 7: ^{13}C NMR spectrum for the butyl branched sample with best fit. The recycle delay was 2 s. The Lorentzian and Gaussian fits to the crystalline and amorphous peaks respectively are also shown.

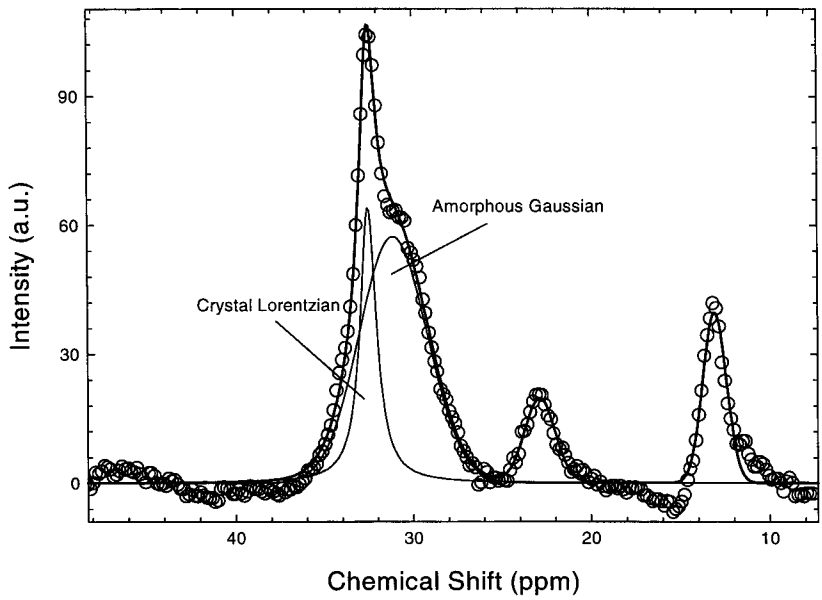

Differences in the time scale of the longitudinal relaxation are shown between the alkane samples in Fig. 8. In order to compare the behaviour of each sample, the data is normalised to account for the effect of lamellar thickness on the recovery of magnetisation, by plotting $M(t)/M_0$ against $t^{1/2}/l$, where l is the lamellar thickness. This is calculated by multiplying the long spacing by the crystallinity. The recovery shows a clear dependence on branching. The linear sample shows the fastest relaxation, the branched samples relaxing more slowly.

Fig. 8: Fraction of recovery of the crystalline peak, against $t^{1/2}/l$, for the alkanes considered. The lines through the data are fits to the reptation model, eqn 3.

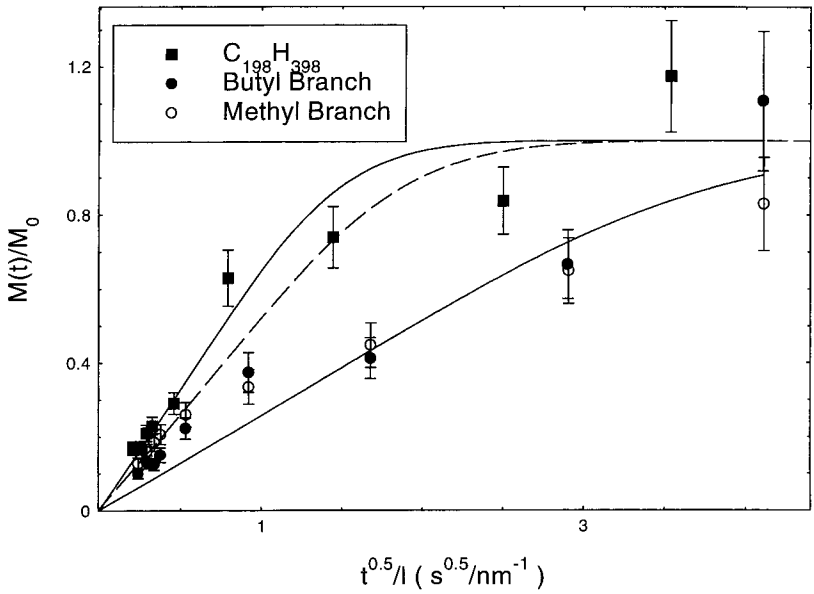

It is not obvious how the addition of a branch point at the fold surface should result in a significant increase in the time scale for the crystalline spin-lattice relaxation. However, the trend of the data can be explained if the origin of the longitudinal relaxation is molecular chain diffusion. Similarly, although spin diffusion in a dilute spin system can be modulated through an abundant spin species[15], the addition of branches at the fold surface should not affect this. The mechanism of magnetisation transport is thus assigned to the solid state diffusion of alkane chains.

Clearly, a branch represents a significant obstacle to the diffusion of a chain through the crystal. It might be expected that the larger the branch, the greater that obstacle to diffusion. If only the data at short recycle delays are considered, such an observation can be made (Fig. 9). It can be seen here that the linear alkane relaxes the most quickly, with the methyl branched sample relaxing significantly more quickly than the butyl branched sample.

Fig. 9: Fraction of recovery of the crystalline peak against $t^{1/2}/l$ for the alkanes considered, recycle delays up to 20 s. The lines through the data are fits to eqn (4).

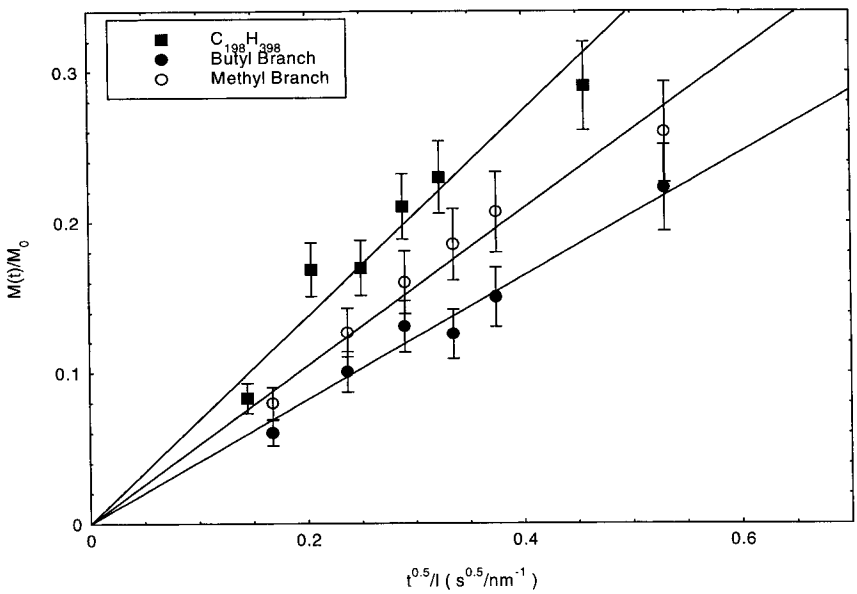

Molecular Chain Diffusion

In order to model the relaxation of magnetisation by solid state diffusion of chains, it is illustrative to consider how this relaxation proceeds. An alkane chain within a lamella of some thickness undergoes a one dimensional random walk along its own axis within the crystal. Whenever a carbon nucleus moves out of the lamella it relaxes. The fraction of magnetisation which has relaxed is, therefore, the fraction of the chain which has left the lamella. This situation is exactly analogous to the situation of a reptating chain in a fixed network[16]. In the tube model for reptation, the situation is reduced to a one dimensional diffusion process. Only the diffusion of the primitive chain is considered, and it is restricted to move only back and forth along itself. In

this case, the fraction of the chain remaining in the tube, ψ, at some time, t, is given by eqn (3)

$$\Psi = \sum_{p;odd} \frac{8}{p^2\pi^2} \exp\left(-\frac{p^2 t}{\tau_D}\right) \qquad (3)$$

Here, τ_D is the reptation time, that is the time needed for the primitive chain to disengage from the tube it was confined to at t = 0. Eqn 3 can alternatively be arrived at by solving the one dimensional Fickian diffusion equation with appropriate boundary conditions[4,17]. Since the experiment measures the amount of magnetisation which has relaxed, and therefore the fraction of the chain which has left the tube, eqn 4 is used to model the relaxation.

$$\frac{M(t)}{M_0} = 1 - \sum_{p;odd} \frac{8}{p^2\pi^2} \exp\left(-\frac{p^2 t}{\tau_D}\right) \qquad (4)$$

This is displayed in Fig. 8. The solid lines represent fits over the whole time range. The dashed line is a fit to the methyl branched sample in the limit of short time, up to 20 s recycle delay. The reptation model satisfactorily represents the relaxation of the linear alkane. It does not satisfactorily represent the relaxation of the branched alkanes. This is not surprising, as the tube model described above does not take into account the effect of constraints to the diffusion process, such as branch points which cannot be accommodated within the crystal.

At short times, eqn 4 satisfactorily represents the relaxation behaviour of all the alkanes, as is displayed in Fig. 9. At longer times, the data from the branched alkanes lie under the short time fit (Fig. 8). This is a result of the much reduced effect of constraints at short times where the longitudinal relaxation is dominated by the free diffusion of polymer chains. Constraints, such as branches, become more significant as the diffusion continues. Nonetheless, constraints still affect the diffusion enough for there to be a significant difference between the samples even in the short time regime.

Diffusion coefficients can be obtained from eqn (4) using eqn (5)[16)]

$$\tau_D = \frac{l^2}{\pi D^2} \qquad (5)$$

Here, l is the lamellar thickness and D is the diffusion coefficient. The diffusion coefficients obtained for the three samples are shown in Table 1, for the short time limit and for the full range of data.

Tab. 1. Diffusion coefficients obtained from eqns 4 and 5.

Alkane	Full Range D (nm^2s^{-1})	Short Time D (nm^2s^{-1})
$C_{198}H_{398}$	0.0847	0.0918
Methyl Branch	0.013	0.053
Butyl Branch	0.016	0.033

The short time diffusion coefficients show a decrease with the addition of a branch and with increase in the length of the branch. There is little difference between the coefficients for the branched alkanes over the full range, though it must be recalled that these originate from fits which were not adequate representations of the data.

The coefficients for the linear alkane show good agreement between the full range result and that in the short time limit, reflecting the satisfactory representation of the full range of data by eqn (4). For the branched alkanes, the longer time data result in a much smaller diffusion coefficient, consistent with the diffusion being suppressed by the branch. The diffusion coefficients obtained for the linear alkane are significantly larger than those obtained by previous workers[4-6)], larger by approximately a factor of 2. The previous work was all on polyethylene systems of much greater molecular weight than the alkanes considered here. In those systems solid state chain diffusion would require a great deal more cooperative motion to progress, so it is not surprising

to find that the diffusion proceeds significantly faster with a much shorter alkane. The results for the branched alkanes are comparable to those measured by Robertson et al.[4] for a polyethylene with crosslinks added at the fold surface.

Conclusions

Monodisperse, ultralong n-alkanes have been characterized and prepared in such a way as they have known folding habits, and that the folding habit is consistent throughout any one particular sample. A progressive saturation pulse sequence has been used to investigate the ^{13}C longitudinal relaxation within the crystalline phase of these samples.

The results obtained were consistent with a solid state diffusion model. Indeed, a reptation model was able to satisfactorily represent the relaxation of the linear alkane. This model satisfactorily represented the relaxation of all the alkanes at short times. The addition of a branch resulted in the decrease of the diffusion constant, with a longer branch producing an even greater decrease. The obtained diffusion coefficients are consistent with those observed for polyethylene by previous workers[4-6].

It is worth noting that although the addition of a branch does lead to a longer relaxation time, the difference is not as large as one might initially expect. Even with the butyl branch sample the relaxation is still relatively fast. This observation is not in disagreement with previous work on solid state chain diffusion. Schmidt-Rohr and Spiess[6] and Robertson et al.[4] both observed that chain diffusion proceeds even in ultra high molecular weight polyethylene (UHMWPE), where remarkably long range dynamic effects are required. These workers also noted that although the addition of crosslinks does inhibit the diffusion, the relaxation is still able to progress even with gel fractions up to 87%. These results suggest that the mobility of chains within crystallites is high, and that such solid state diffusion is a powerful enough process to overcome even relatively large obstacles to its progress. This could lead to some interesting consequences in the field of ordering, structure and dynamics in semicrystalline polymers.

References

[1] P. G. De Gennes, *"Scaling Concepts in Polymer Physics"*, Cornell University Press, (1979)

[2] D. E. Axelson, L. Mandelkern, R. Popli, P. Mathieu, *J. Polym. Sci., Polym. Phys.* **21**, 2319, (1983)

[3] B. Schroter, A. Posern, *Makromol. Chem., Rapid Commun.* **3**, 623 (1982)

[4] M. B. Robertson, I. M. Ward, P. G. Klein, K. J. Packer, *Macromolecules* **30**, 6893, (1997)

[5] I. J. Colquhoun, K. J. Packer, *Brit. Polym. J.* **19**, 151, (1987)

[6] K. Schmidt-Rohr, H. W. Spiess, *Macromolecules* **24**, 5288, (1991)

[7] J. D. Hoffman, G. Williams, E. Passaglia, *J. Polym. Sci.* **C14**, 173, (1966)

[8] J. L. Syi, M. L. Mansfield, *Polymer* **29**, 987, (1988)

[9] G. Ungar, J. Stejny, A. Keller, I. Bidd, M.C. Whiting, *Science* **229**, 386, (1985)

[10] G. M. Brooke, S. Burnett, S. Mohammed, D. Proctor, M.C. Whiting, *J. Chem. Soc., Perkin Trans. 1* **13**, 1635, (1996)

[11] E. D. Becker, J. A. Ferretti, P. N. Gambhir, *Anal. Chem.* **51**, 1413, (1979)

[12] G. Ungar, A. Keller, *Polymer* **27**, 1835, (1986)

[13] S. J. Organ, A. Keller, *J. Polym. Sci., Polym. Phys.* **25**, 2409, (1987)

[14] G. Ungar, S. J. Organ, A. Keller, *J. Polym. Sci., Polym. Lett.* **26**, 259, (1988)

[15] P. Robyr, M. Tomaselli, J. Straka, C. Grob-Pisano, U. W. Suter, B. H. Meier, R. R. Ernst, *Molec. Phys.* **84**, 995, (1995)

[16] M. Doi, S. F. Edwards, *"The Theory of Polymer Dynamics"*, Clarendon Press, Oxford, (1986)

[17] J. Crank, *"The Mathematics of Diffusion"*, Clarendon Press, Oxford, (1975)